SEMARAK ILMU PUBLISHING

Journal of Advanced Research in Fluid Mechanics and Thermal Sciences

Journal homepage:
https://semarakilmu.com.my/journals/index.php/fluid_mechanics_thermal_sciences/index
ISSN: 2289-7879

# Effect of Thermophoresis and Heat Source on Unsteady Hydromagnetic Free Convective Fluid Flow Embedded in a Porous Material

Shaik Nuslin Bibi[1,*], Gunampalle Padma[2], Sagi Lalitha[1], Puliyeddula Sarada[1]

[1] Department of Freshman Engineering, Geethanjali College of Engineering and Technology, Telangana, India
[2] Department of Mathematics, Vardhaman College of Engineering, Hyderabad, Telangana, India

**ARTICLE INFO**

***Article history:***
Received 8 June 2024
Received in revised form 14 September 2024
Accepted 22 September 2024
Available online 10 October 2024

***Keywords:***
Soret effect; radiative heat flux; heat source; MHD; finite element method

**ABSTRACT**

The present research paper aims to study the Soret effect and Heat source Radiation effect on a Magneto Hydro Dynamics fluid through a vertical fluctuating porous plate. Dimensional non-linear coupled differential equations altered into dimensional less by introducing similarity variables. Time-dependent suction is assumed and the radiative flux is described using the differential approximation for radiation. The Galerkin finite element method is used to sole the equations governing flow. The flow phenomenon has been characterized with the help of flow parameters such as velocity, temperature and concentration profiles for different parameters such as $S_C, P_\Gamma, M, Q, K, N_\Gamma, K_\Gamma, G_m, S_O, E_C$ and $G_\Gamma$. Schmidt number, Prandtl number, Magnetic field, Heat source, Permeability parameter, Thermal radiation, Chemical reaction, Solutal Grashof number, Soret number, Eckert number and Grashof number. The velocity, temperature and concentration are shown graphically. The coefficient of skin-friction, Nusselt number and Sherwood number are shown in tables.

## 1. Introduction

The problem of fluid in an electromagnetic field has been studies for its importance in geophysics, metallurgy and aerodynamic extrusion of plastic sheets and other engineering process such as in petroleum engineering, chemical engineering, composite or ceramic engineering and heat dealing with heat flow and mass transfer over a vertical porous plate with variable suction, heat absorption. The phenomenon of heat and mass transfer is observed in buoyancy induced motions in the atmosphere, in bodies of water, quasi – solid bodies, such as earth and so on.

Numerical study on the parabolic flow of MHD fluid past a vertical plate in a porous Medium is studied by Sivaiah *et al.,* [1] and Reddy *et al.,* [2]. In many mass transfer processes, Appearances of MHD three-dimensional flow of nanofluid over a permeable stretching porous [3,4]. Several studies have been carried out on Numerical study of MHD boundary layer flow of a viscoelastic and dissipative fluid past a porous plate in the presence of thermal radiation, while others have

[*] *Corresponding author.*
*E-mail address: nuslinsk@gmail.com*

https://doi.org/10.37934/arfmts.122.1.94106

investigated the unsteady cases, such as unsteady MHD convection heat transfer past a semi-infinite vertical porous moving plate with variable suction [5-8]. Raptis conversed the Flow of a micro polar fluid past continuously moving plate in presence of radiation [9,10]. Suneetha *et al.,* [11] presented Radiation and mass transfer effects on MHD free convective dissipative fluid in the occurrence of heat source/sink. Anand Rao and Raju [12] discussed the Effects of hall current, Soret and Dufour on an unsteady MHD flow and Heat transfer along a porous flat plate with mass transfer. Srihari *et al.,* [13] and Abbas and Hayat [14] discussed Hall effect on MHD flow along a porous flat plate with Mass transfer and source/sink, Reddy and Makinde [15-17] and Reddy *et al.,* [18] discussed Buoyancy and chemical reaction effects on MHD mixed convection heat and mass transfer in a porous medium with thermal radiation. Hamrelaine *et al.,* [19], Ismail *et al.,* [20], and Bakar *et al.,* [21] discussed Soret and Dufer effects on unsteady MHD flow past an infinite vertical porous plate with thermal radiation.

In the present paper, effect of thermal radiation, time-dependent suction and chemical reaction on the two-dimensional flow of an incompressible Boussinseq' s fluid in the presence of uniform magnetic field applied normal to the flow has been studied. The problem is governed by the system of coupled non-linear partial differential equations whose exact solutions are difficult to obtain, if possible. So, Galerkin finite element method has been adopted for its solution, which is more economical from computational point view.

## 2. Methodology: Mathematical Analysis

Consider the problem of unsteady two-dimensional, laminar, boundary layer flow of a viscous, incompressible, electrically conducting fluid along a semi-infinite vertical plate in the presence of thermal and concentration buoyancy effects as shown in Figure 1. Time dependent suction is considered normal to the flow. The $Y'$ -axis is taken along the plate in the direction of the flow and $X'$ -axis normal to it. Further, due to the semi-infinite plane surface assumption the flow variables are the functions of normal distances $X'$ and $t'$ only. A uniform magnetic field is applied normal to the direction of the flow. Now, under the usual Boussinesq's approximation.

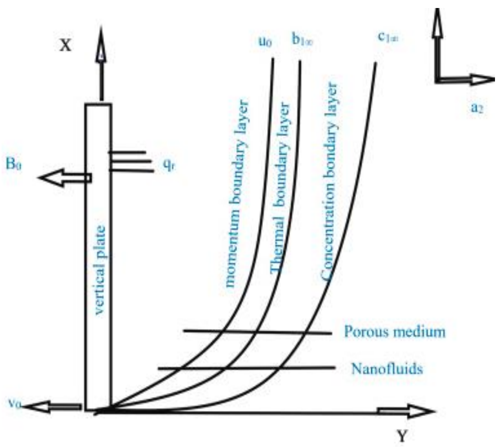


**Fig. 1.** Schematic Diagram of the Problem

The governing equations of the flow problem are

Continuity equation:

$$\frac{\partial v\prime}{\partial y\prime} = 0 \tag{1}$$

Momentum equation:

$$\frac{\partial u'}{\partial t'} + v'\frac{\partial u'}{\partial y'} = g\beta(T' - T'_\infty) + g\beta^*(C' - C'_\infty) + v\frac{\partial^2 u'}{\partial y'^2} - \frac{v}{K'}u' - \frac{\sigma B_O^2}{\rho'}u' \quad (2)$$

Energy Equation:

$$\frac{\partial T'}{\partial t'} + v'\frac{\partial T'}{\partial y'} = \frac{k}{\rho c_p}\frac{\partial^2 T'}{\partial y'^2} - \frac{1}{\rho c_p}\frac{\partial q'_r}{\partial y'} - \frac{Qo}{\rho c_p}(T' - T'_\infty) \quad (3)$$

Concentration Equation:

$$\frac{\partial C'}{\partial t'} + v'\frac{\partial C'}{\partial y'} = v\frac{\partial^2 C'}{\partial y'^2} + \frac{D_m k_T}{T_m}\frac{\partial^2 T'}{\partial y'^2} \quad (4)$$

The boundary conditions for the velocity, temperature and concentration fields are

$$t > 0, u' = u_o, T' = T'_\infty + \varepsilon(T'_W - T'_\infty)e^{n't'}, C' = C'_\infty + \varepsilon(C'_W - C'_\infty)e^{n't'} at y' = 0$$

$$u' \to 0,\ \ T' \to T'_\infty,\quad C' \to C'_\infty, as\ \ y' \to \infty \quad (5)$$

where $T'_W$ and $C'_W$ Dimensional temperature and concentration respectively, $T'_W$ and $C'_W$ are the free stream Dimensional temperature and concentration respectively.

The radiative heat flux term by using the Rosseland approximation is given by

$$q'_r = -\frac{4\sigma'}{3k'_1}\frac{\partial T'^4}{\partial y'} \quad (6)$$

All the variables are defined in the nomenclature. It is assumed that the temperature differences within the flow are sufficiently small so that $T^4$ can be expanded in a Taylor series about the free stream temperature $T_\infty$ so that after rejecting higher order terms

$$T^4 \approx 4T'^3_\infty T' - 3T'^4_\infty \quad (7)$$

The energy equation after substitution of Eq. (6) and Eq. (7) can now be written as

$$\frac{\partial T'}{\partial t'} + v'\frac{\partial T'}{\partial y'} = \frac{k}{\rho c_p}\frac{\partial^2 T'}{\partial y'^2} + \frac{16\sigma' T_\infty^3}{3\rho c_p k'}\frac{\partial^2 T'}{\partial y'^2} - Q_o(T' - T'_\infty) \quad (8)$$

From Eq. (1) one can see that the suction is a function of time only. Hence, it is assumed to be in the following form:

$$v' = -V_O(1 + \varepsilon A e^{n't'}) \quad (9)$$

where $A$ is the suction parameter and$\varepsilon A << 1$. Here $V_O$is mean suction velocity, which is a non-zero positive constant and the minus sign indicates that the suction is towards the plate. It is now convenient to introduce the following dimensionless parameters:

$$u = \frac{u'}{U_o}, y = \frac{U_o y\prime}{v}, t = \frac{t\prime U_o^2}{v}, P_\Gamma = \frac{\rho c_p v}{k}, S_c = \frac{v}{D}, \theta = \frac{T' - T'_\infty}{T'_w - T'_\infty}, \varphi = \frac{C' - C'_\infty}{C'_w - C'_\infty}, K = \frac{K\prime U_o^2}{v^2},$$

$$n = \frac{vn'}{U_o^2}, G_\Gamma = \frac{g\beta v(T\prime_w - T\prime_\infty)}{U_o^3}, G_C = \frac{vg\beta * (C'_w - C'_\infty)}{U_o^3}, Q = \frac{Q_o v}{U_o^2}, M = \frac{\sigma B_o^2 v}{\rho U_o^2}, K_\Gamma^2 = \frac{K_\Gamma^2 v}{U_o^2}$$

$$S_O = \frac{D_m k_T (T'_w - T'_\infty)}{v T_m (C\prime_w - C\prime_\infty)}, E_C = \frac{{v'_o}^2}{C_p (T'_w - T'_\infty)}, N_\Gamma = \frac{16\sigma' T_\infty^3}{3k'k} \tag{10}$$

On substituting of Eq. (9) into Eq. (2), Eq. (4) and Eq. (7), the following governing equations are obtained in non-dimensional form

$$\frac{\partial u}{\partial t} - (1 + \varepsilon A e^{nt}) \frac{\partial u}{\partial y} = G_\Gamma \theta + G_m \varphi + \frac{\partial^2 u}{\partial y^2} - \left(M + \frac{1}{K}\right) u \tag{11}$$

$$\frac{\partial \theta}{\partial t} - (1 + \varepsilon A e^{nt}) \frac{\partial \theta}{\partial y} = \left(\frac{1 + N_\Gamma}{P_\Gamma}\right) \frac{\partial^2 \theta}{\partial y^2} - Q\theta \tag{12}$$

$$\frac{\partial \varphi}{\partial t} - (1 + \varepsilon A e^{nt}) \frac{\partial \varphi}{\partial y} = \frac{1}{S_C} \frac{\partial^2 \varphi}{\partial y^2} + So \frac{\partial^2 \theta}{\partial y^2} \tag{13}$$

The corresponding boundary conditions are

$$u = 1, \theta = 1 + \varepsilon e^{nt}, \varphi = 1 + \varepsilon e^{nt} \quad on \quad y = 0$$

$$u \to 0, \theta \to 0, \varphi \to 0 \quad as \quad y \to \infty \tag{14}$$

The mathematical formulation of the problem is now completed. Eq. (11) to Eq. (13) are coupled non-linear systems of partial differential equations, and are to be solved by using the initial and boundary conditions given in Eq. (14). However, exact solutions are difficult if possible. Hence these equations are solved by Galerkin finite element method.

### *2.1 Method of Solution*

Applying the Galerkin finite element method for Eq. (11). Over the element (*e*) $(y_j \le y \le y_k)$ is

$$\int_{y_J}^{y_K} N^{(e)^T} \left( \frac{\partial^2 u^{(e)}}{\partial y^2} + B \frac{\partial u^{(e)}}{\partial y} - \frac{\partial u^{(e)}}{\partial t} - N u^{(e)} + R_1 \right) dy = 0 \tag{15}$$

where

$$B = 1 + \varepsilon A e^{nt} \qquad R_1 = G_\Gamma \theta + G_m \varphi \qquad N = M + \frac{1}{K}$$

Let the linear piecewise approximation solution

$$u^{(e)} = N_j(y) u_j(t) + N_k(y) u_k(t) = N_j u_j + N_k u_k$$

where

$$N_j = \frac{y_k - y}{y_k - y_j} \qquad N_k = \frac{y - y_j}{y_k - y_j} \qquad N^{(e)^T} = \begin{bmatrix} N_j & N_k \end{bmatrix}^T = \begin{bmatrix} N_j \\ N_k \end{bmatrix}$$

The Galerkin expansion for the differential equation (15) becomes

$$\left. N^{(e)^T} \frac{\partial u^{(e)}}{\partial y} \right\}_{y_j}^{y_K} - \int_{y_j}^{y_K} \left\{ \frac{\partial N^{(e)^T}}{\partial y} \frac{\partial u^{(e)}}{\partial y} - N^{(e)^T} \left( B \frac{\partial u^{(e)}}{\partial y} + \frac{\partial u^{(e)}}{\partial t} + N u^{(e)} - R_1 \right) \right\} dy = 0 \tag{16}$$

Neglecting the first term in Eq. (16) we get

$$\int_{y_j}^{y_K} \left\{ \frac{\partial N^{(e)^T}}{\partial y} \frac{\partial u^{(e)}}{\partial y} - N^{(e)^T} \left( B \frac{\partial u^{(e)}}{\partial y} - \frac{\partial u^{(e)}}{\partial t} - N u^{(e)} + R_1 \right) \right\} dy = 0$$

$$\frac{1}{l^{(e)}} \begin{bmatrix} 1 & -1 \\ -1 & 1 \end{bmatrix} \begin{bmatrix} u_j \\ u_k \end{bmatrix} - \frac{B}{2} \begin{bmatrix} -1 & 1 \\ -1 & 1 \end{bmatrix} \begin{bmatrix} u_j \\ u_k \end{bmatrix} + \frac{l_{(e)}}{6} \begin{bmatrix} 2 & 1 \\ 1 & 2 \end{bmatrix} \begin{bmatrix} u_j^{\bullet} \\ u_k^{\bullet} \end{bmatrix} + \frac{N l^{(e)}}{6} \begin{bmatrix} 2 & 1 \\ 1 & 2 \end{bmatrix} \begin{bmatrix} u_j \\ u_k \end{bmatrix} = R_1 \frac{l_{(e)}}{2} \begin{bmatrix} 1 \\ 1 \end{bmatrix}$$

Where $l^{(e)} = y_k - y_j = h$and dot denotes the differentiation with respect to $t$.

We write the element equations for the elements $y_{i-1} \le y \le y_i$ and $y_j \le y \le y_k$ assemble three element equations, we obtain

$$\frac{1}{l^{(e)^2}} \begin{bmatrix} 1 & -1 & 0 \\ -1 & 2 & -1 \\ 0 & -1 & 1 \end{bmatrix} \begin{bmatrix} u_{i-1} \\ u_i \\ u_{i+1} \end{bmatrix} - \frac{B}{2 l^{(e)}} \begin{bmatrix} -1 & 1 & 0 \\ -1 & 0 & 1 \\ 0 & -1 & 1 \end{bmatrix} \begin{bmatrix} u_{i-1} \\ u_i \\ u_{i+1} \end{bmatrix} + \frac{1}{6} \begin{bmatrix} 2 & 1 & 0 \\ 1 & 4 & 1 \\ 0 & 1 & 2 \end{bmatrix} \begin{bmatrix} u_{i-1}^{\bullet} \\ u_i^{\bullet} \\ u_{i+1}^{\bullet} \end{bmatrix} +$$
$$\frac{N}{6} \begin{bmatrix} 2 & 1 & 0 \\ 1 & 4 & 1 \\ 0 & 1 & 2 \end{bmatrix} \begin{bmatrix} u_{i-1} \\ u_i \\ u_{i+1} \end{bmatrix} = \frac{R_1}{2} \begin{bmatrix} 1 \\ 2 \\ 1 \end{bmatrix} \tag{17}$$

Now put row corresponding to the node *i* to zero, from Eq. (17) the difference schemes is

$$\frac{1}{l^{(e)^2}} [-u_{i-1} + 2u_i - u_{i+1}] - \frac{B}{2 l^{(e)}} [-u_{i-1} + u_{i+1}] + \frac{1}{6} [u_{i-1}^{\bullet} + 4u_i^{\bullet} + u_{i+1}^{\bullet}] + \frac{N}{6} [u_{I-1} + 4u_i + u_{i+1}] = R_1$$

Applying the Trapezoidal rule, following system of equations in Crank-Nicholson method are obtained:

$$A_1 u_{i-1}^{j+1} + A_2 u_i^{j+1} + A_3 u_{i+1}^{j+1} = A_4 u_{i-1}^{j} + A_5 u_i^{j} + A_6 u_{i+1}^{j} + R^* \tag{18}$$

where

$$A_1 = 2 - 6r + 3Brh + Nk \qquad A_2 = 8 + 12r + 4Nk \qquad A_3 = 2 - 6r - 3Brh + Nk$$

$$A_4 = 2 + 6r - 3Brh - Nk \qquad A_5 = 8 - 12r - 4Nk \qquad A_6 = 2 + 6r + 3Brh - Nk$$

$$R^* = 12(G_\Gamma) k \theta_i^j + 12(G_m) k \phi_i^j$$

Applying similar procedure to Eq. (12) and Eq. (13) then we get

$$B_1\theta_{i-1}^{j+1} + B_2\theta_i^{j+1} + B_3\theta_{i+1}^{j+1} = B_4\theta_{i-1}^{j} + B_5\theta_i^{j} + B_6\theta_{i+1}^{j} \tag{19}$$

$$C_1\varphi_{i-1}^{j+1} + C_2\varphi_i^{j+1} + C_3\varphi_{i+1}^{j+1} = C_4\varphi_{i-1}^{j} + C_5\varphi_i^{j} + C_6\varphi_{i+1}^{j} \tag{20}$$

where

$$B_1 = 2 - 6Dr + 3Brh + Qk \qquad B_2 = 8 + 12Dr + 4Qk$$
$$B_3 = 2 - 6Dr - 3Brh + Qk \qquad B_4 = 2 + 6Dr - 3Brh - Qk$$
$$B_5 = 8 - 12Dr - Qk \qquad B_6 = 2 + 6Dr + 3Brh - Qk$$

$$R^{**} = 12rE_C(u[i+1] - u[i])^2$$

$$C_1 = 2S_C - 6r + 3BS_Crh + ES_Ck \qquad C_2 = 8S_C + 12r + ES_Ck$$
$$C_3 = 2S_C - 6r - 3BS_Crh + ES_Ck \qquad C_4 = 2S_C + 6r - 3BS_Crh - ES_Ck$$
$$C_5 = 8S_C - 12r - 4ES_Ck \qquad C_6 = 2S_C + 6r + 3BS_Crh - ES_Ck$$

$$R^{***} = 12rS_CS_o(\theta[i-1] - 2\theta[i] + \theta[i+1])$$

Here $r = \frac{k}{h^2}$, $D = \frac{1+N_\Gamma}{P_\Gamma}$, $E = K_\Gamma^2$ and $h, k$ are the mesh sizes along $y$ -direction and time $t$ -direction respectively. Index $i$ refers to the space and $j$ refers to the time. In Eq. (18) to Eq. (20), taking $i$ = 1(1) $n$ and using initial and boundary conditions (14), the following system of equations are obtained:

$$A_iX_i = B_i \qquad i = 1(1)3 \tag{21}$$

where $A_i$'s are matrices of order $n$ and $X_i, B_i$'s column matrices having $n$ – components. The solutions of above system of equations are obtained by using Thomas algorithm for velocity, temperature and concentration. Also, numerical solutions for these equations are obtained by C-program. In order to prove the convergence and stability of finite element method, the same C-program was run with slightly changed values of *h* and *k* and no significant change was observed in the values of $u$, $\theta$and $\varphi$. Hence, the finite element method is stable and convergent.

### *2.2 Skin Friction*

The skin-friction, Nusselt number and Sherwood number are important physical parameters for this type of boundary layer flow. The skin friction, rate of heat and mass transfer are

Skin friction coefficient ($C_f$) is given by $C_f = \left(\frac{\partial u}{\partial y}\right)_{y=0}$ (22)

Nusselt number ($Nu$) at the plate is $Nu = \left(\frac{\partial \theta}{\partial y}\right)_{y=0}$ (23)

$Nu = 0.664\ (Re)0.5(Pr)0.33$

Sherwood number ($Sh$) at the plate is $Sh = \left(\frac{\partial \varphi}{\partial y}\right)_{y=0}$ (24)

## 3. Results

The formulation of the problem that accounts for the effects of the chemical reaction on an unsteady MHD flow past a semi-infinite vertical porous plate with viscous dissipation is performed in the preceding sections. The governing equations of the flow field are solved analytically by using a finite element method. The expressions for the velocity, temperature, concentration, skin-friction, Nusselt number, and Sherwood number are obtained. To get a physical insight of the problem, the above physical quantities are computed numerically for different values of the governing parameters, viz., the thermal Grashof number $G_{\Gamma}$, the solutal Grashof number $G_m$, the magnetic parameter $M$, the thermal radiation the permeability parameter $K$, the Prandtl number $P_{\Gamma}$, the heat source parameter $Q$, the Eckert number $E_C$, the Schmidt number $S_C$, the chemical reaction parameter $K_{\Gamma}$, the soret numder $S_O$ . Here we fixed $\varepsilon = 0.02, n = 0.5, t = 1.0$.

Figure 2(a) and Figure 2(b) illustrate the velocity and temperature profiles for different values of Heat source parameter $Q$, the numerical results show that the effect of increasing values of heat source parameter result in a decreasing velocity and temperature.

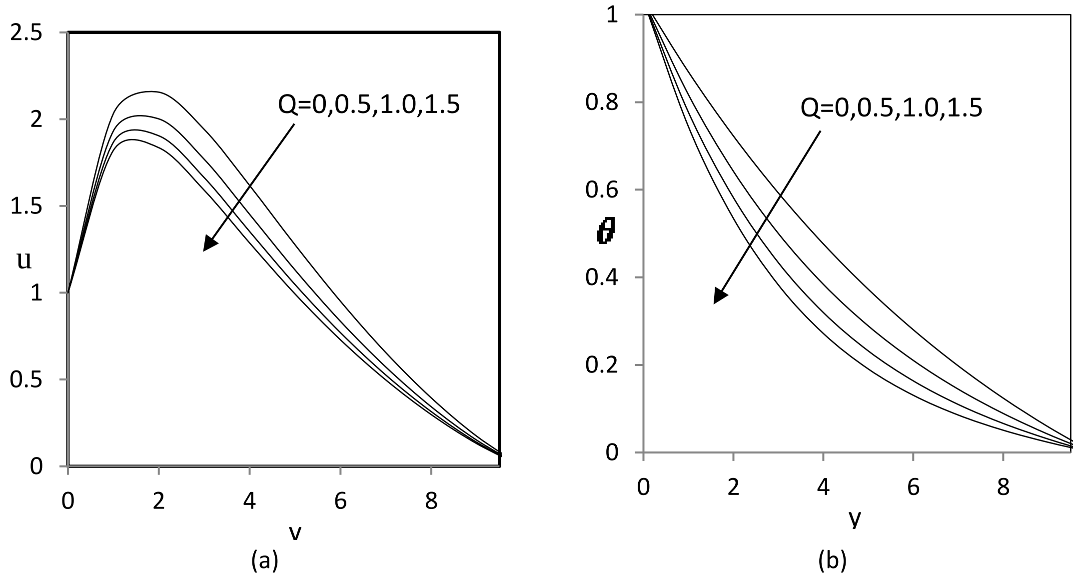


**Fig. 2.** Effects of $Q$ on (a) Velocity and (b) Temperature profile
$\begin{pmatrix} S_C = 0.22, \varepsilon = 0.02, P_{\Gamma} = 0.71, M = 0.5, G_{\Gamma} = 5, G_C = 5, S_O = 1, \\ K_{\Gamma} = 0.5, K = 1, E_C = 0.001, t = 1.0, N_{\Gamma} = 0.5, n = 0.5, A = 0.3 \end{pmatrix}$

Figure 3(a) and Figure 3(b) illustrate the behavior Velocity and Temperature for different values of Thermal radiation parameter $N_{\Gamma}$ . It is observed that an increase in $N_{\Gamma}$ contributes to increase in both the values of velocity and Temperature.

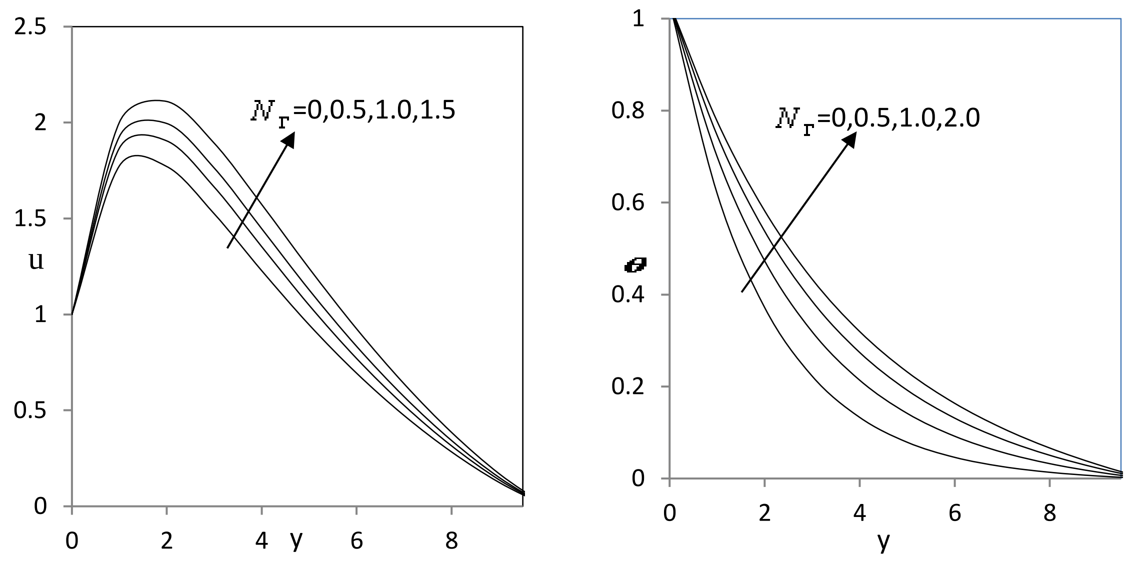


(a) (b)

**Fig. 3.** Effects of $N_\Gamma$ on (a) Velocity and (b) Temperature profile

$$\begin{pmatrix} S_C = 0.22, \varepsilon = 0.02, P_\Gamma = 0.71, M = 0.5, G_\Gamma = 5, G_m = 5, S_O = 1, \\ K_\Gamma = 0.5, K = 1, E_C = 0.001, t = 1.0, Q = 1, n = 0.5, A = 0.3 \end{pmatrix}$$

The influence of the solutel Grashof number Gm on the velocity is presented in Figure 4. It is observed that, while all other parameters are held constant and velocity increases with an increase in solute Grashof number $G_m$.

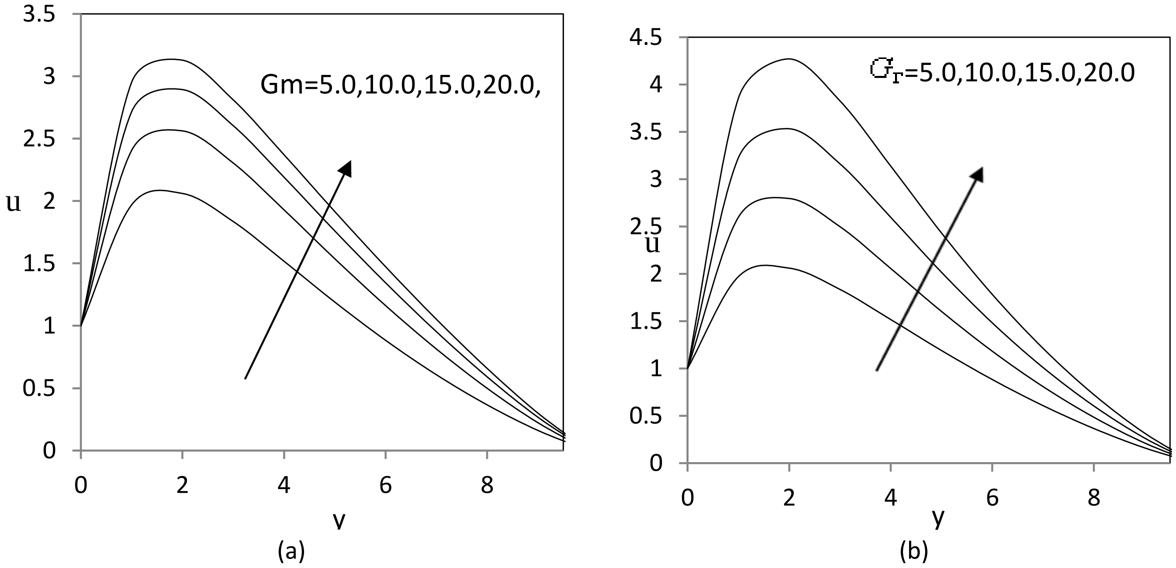


(a) (b)

**Fig. 4.** Effects of $G_m$ $and$ $Gr$ on Velocity

$$\begin{pmatrix} S_C = 0.22, \varepsilon = 0.02, P_\Gamma = 0.71, M = 0.5, N_\Gamma = 0.5, G_\Gamma = 5, \\ S_O = 1, K = 1, E_C = 0.001, t = 1.0, Q = 1, n = 0.5, A = 0.3 \end{pmatrix}$$

Figure 5(a) and Figure 5(b) illustrate the velocity and temperature profiles for different values of the Prandtl number $P_\Gamma$. The Prandtl number defines the ratio of momentum diffusivity to thermal diffusivity. The numerical results show that the effect of increasing values of Prandtl number results in a decreasing velocity (Figure 5(a)). From Figure 5(b), it is observed that an increase in the Prandtl number results a decrease of the thermal boundary layer thickness and in general lower average temperature within the boundary layer.

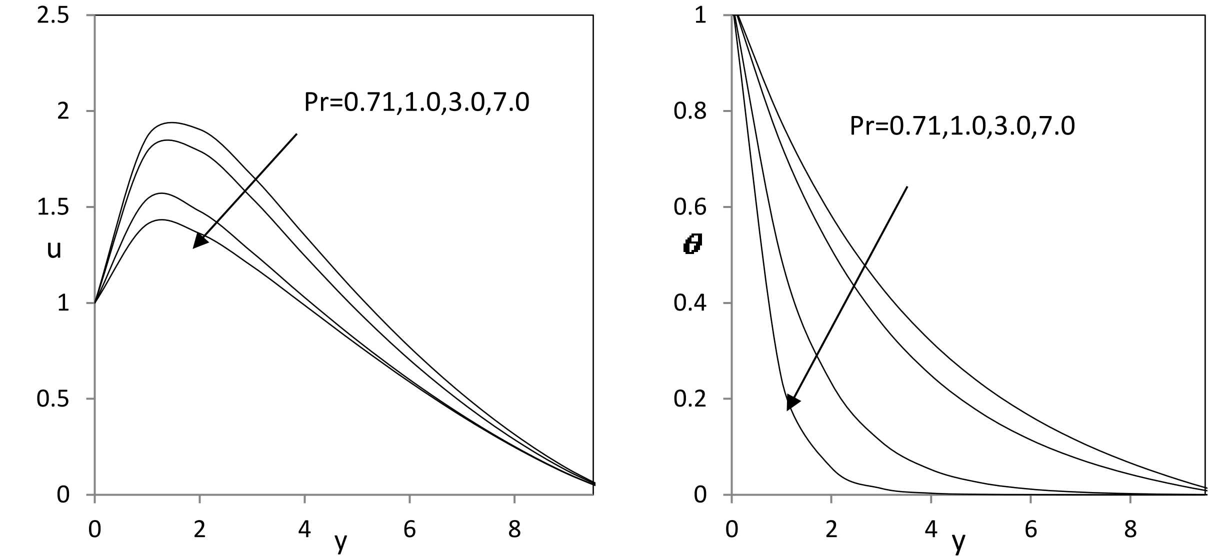


(a) (b)

**Fig. 5.** Effects of $P_\Gamma$ on (a) Velocity and (b) Temperature profile

$$\begin{pmatrix} S_C = 0.22, \varepsilon = 0.02, Q = 1, M = 0.5, G_\Gamma = 5, G_m = 5, S_O = 1, \\ K_\Gamma = 0.5, K = 1, E_C = 0.001, t = 1.0, N_\Gamma = 0.5, n = 0.5, A = 0.3 \end{pmatrix}$$

For various values of the magnetic parameter $M$, the velocity profiles are plotted in Figure 6. It can be seen that as $M$ increases, the velocity decreases. This result qualitatively agrees with the expectations, since the magnetic field exerts a retarding force on the flow.

The effect of the permeability parameter $K$ on the velocity field is shown in Figure 7. An increase in the resistance of the porous medium which will tend to increase the velocity.

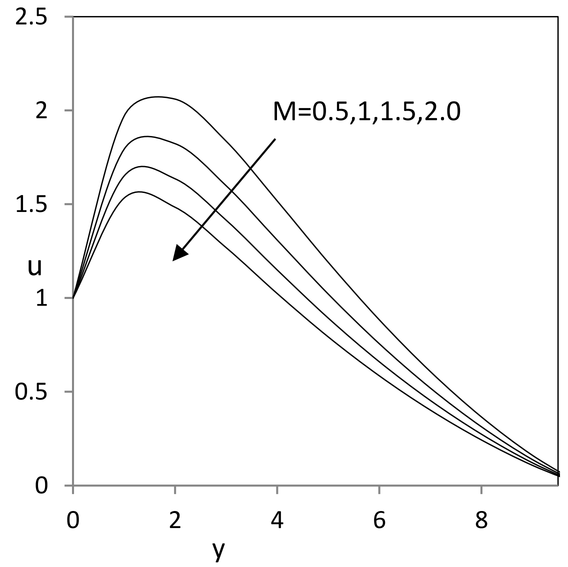


**Fig. 6.** Effects of $M$ on Velocity

$$\begin{pmatrix} S_C = 0.22, \varepsilon = 0.02, P_\Gamma = 0.71, G_\Gamma = 5, N_\Gamma = 0.5, G_m = 5, \\ S_O = 1, K = 1, E_C = 0.001, t = 1.0, Q = 1, n = 0.5, A = 0.3 \end{pmatrix}$$

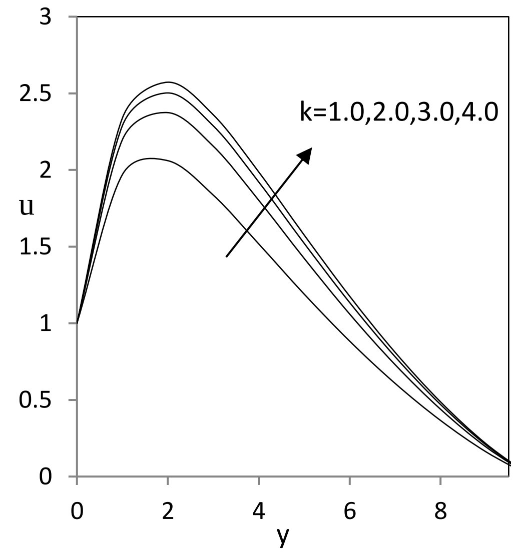


**Fig. 7.** Effects of $K$ on Velocity

$$\begin{pmatrix} S_C = 0.22, \varepsilon = 0.02, P_\Gamma = 0.71, M = 0.5, N_\Gamma = 0.5, G_\Gamma = 5, \\ S_O = 1, G_m = 5, E_C = 0.001, t = 1.0, Q = 1, n = 0.5, A = 0.3 \end{pmatrix}$$

Figure 8(a) and Figure 8(b) respectively. The Schmidt number embodies the ratio of the momentum to the mass diffusivity. The Schmidt number $S_C$ therefore quantifies the relative effectiveness of momentum and mass transport by diffusion in the hydrodynamic (velocity) and concentration (species) boundary layers. As the Schmidt number $S_C$ increases the concentration and velocity decreases.

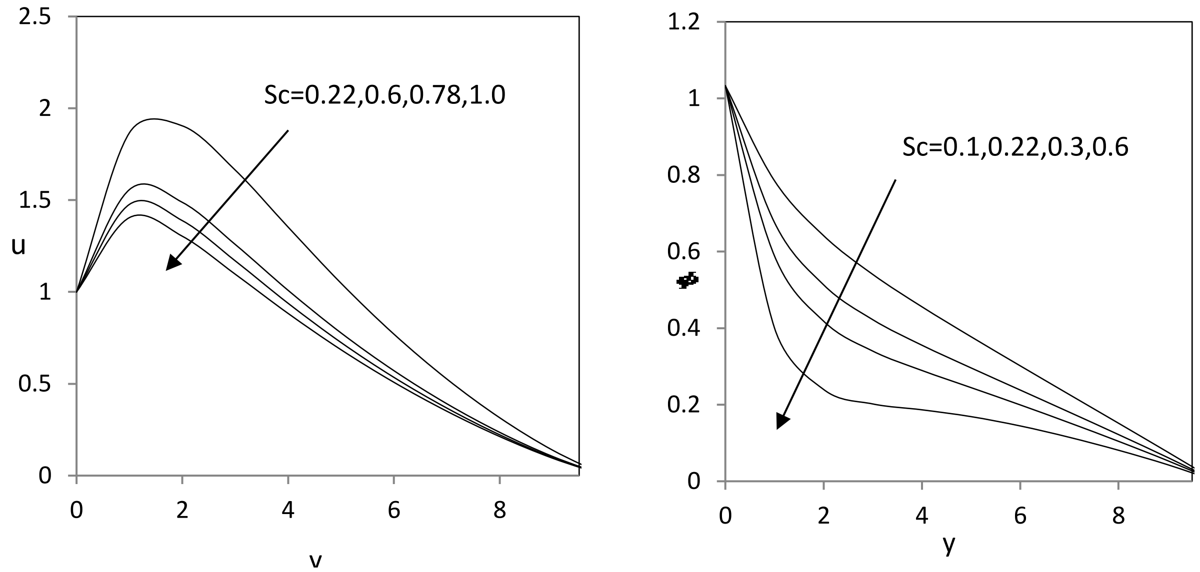


(a) (b)

**Fig. 8.** Effects of $S_C$ on (a) Velocity and (b) Concentration profile
$\begin{pmatrix} P_\Gamma = 0.71, \varepsilon = 0.02, Q = 1, M = 0.5, G_\Gamma = 5, G_m = 5, S_O = 1, \\ K_\Gamma = 0.5, K = 1, E_C = 0.001, t = 1.0, N_\Gamma = 0.5, n = 0.5, A = 0.3 \end{pmatrix}$

Figure 9(a) and Figure 9(b) describe the velocity and concentration profiles for diverse values of the Soret number $S_O$. The Soret number defines the ratio of temperature difference to the concentration It is noticed that a growth in the Soret number reduction in the velocity and concentration within the boundary layer.

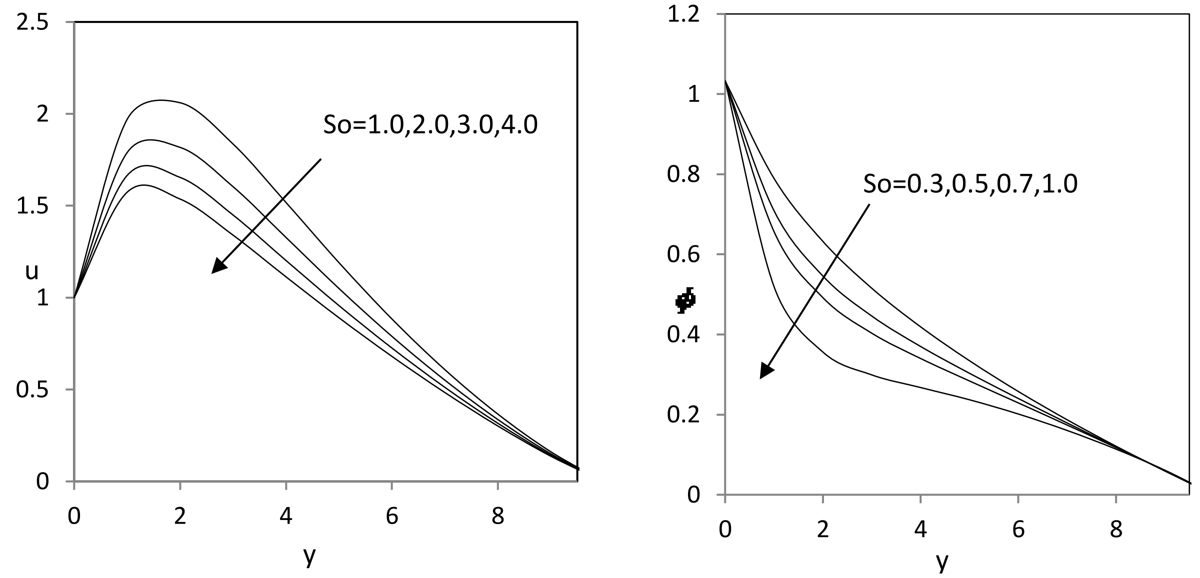


(a) (b)

**Fig. 9.** Effects of $S_O$ on (a) velocity and (b) concentration profile
$\begin{pmatrix} P_\Gamma = 0.71, \varepsilon = 0.02, Q = 1, M = 0.5, G_\Gamma = 5, G_m = 5, S_C = 0.22, \\ K_\Gamma = 0.5, K = 1, E_C = 0.001, t = 1.0, N_\Gamma = 0.5, n = 0.5, A = 0.3 \end{pmatrix}$

The effects of several governing parameters on the skin friction coefficient $C_f$, Nusselt number $Nu$ and the Sherwood number $Sh$ are shown in Table 1, Table 2 and Table 3. From Table 1, it is noticed that as $G_m$ increases, the skin friction coefficient increases. It is obvious that as $M$ or $K$ increases, the skin friction coefficient decreases. From Table 2, it is noticed that rise in the $Q$ or the $P_\Gamma$ Prandtl number reduces the skin friction and increases the Nusselt number. Also, it is found that as $Ec$ and $Nr$ increases the skin friction increases and the Nusselt number increases. From Table 3, it is found that as $S_C$ increases, the skin friction coefficient reduced and the Sherwood number decreases. Also, it is found that as $So$ increases the skin friction growth and the Sherwood number increases.

**Table 1**
Effect of $Gm$, $M$ and $K$ on $C_f$ ($N_\Gamma$ = 0.5, $Q$ = 1.0, $\mathrm{Pr}$ = 0.71, $Ec$ = 0.001, $Sc$ = 0.22, $So$ = 1.0, $K_\Gamma$ = 0.5)

| $Gm$ | $M$ | $K$ | $C_f$ |
|---|---|---|---|
| 5.0 | 0.5 | 1.0 | 3.7681 |
| 5.0 | 0.5 | 1.0 | 4.9583 |
| 10.0 | 0.5 | 1.0 | 4.2746 |
| 5.0 | 1.0 | 1.0 | 2.3275 |
| 5.0 | 0.5 | 2.0 | 2.9958 |

**Table 2**
Effect of $Q$, $\mathrm{Pr}$, $N_\Gamma$ and $Ec$ on $C_f$ and $Nu$ ($Gm$ = 5.0, $M$ = 0.5, $K$ = 1.0, $Sc$ = 0.22, $So$ = 1.0)

| $Q$ | $\mathrm{Pr}$ | $N_\Gamma$ | $C_f$ | $Nu$ |
|---|---|---|---|---|
| 1.0 | 0.71 | 0.5 | 3.7681 | 1.6513 |
| 2.0 | 0.71 | 0.5 | 3.1542 | 1.5324 |
| 1.0 | 7.0 | 0.5 | 2.8564 | 1.1258 |
| 1.0 | 0.71 | 1.0 | 4.2654 | 2.5413 |
| 1.0 | 0.71 | 0.5 | 3.8916 | 1.8645 |

**Table 3**
Effect of $Sc$ , $So$ and $K_\Gamma$ on $C_f$ and $Sh$ ($Gm$ = 5.0, $M$ = 0.5, $K$ = 1.0, $Q$ = 1.0, $\mathrm{Pr}$ = 0.71, $N_\Gamma$ = 0.5)

| $Sc$ | $So$ | $C_f$ | $Sh$ |
|---|---|---|---|
| 0.22 | 1.0 | 3.7681 | 1.4256 |
| 0.60 | 1.0 | 3.2132 | 1.2546 |
| 0.22 | 2.0 | 3.9245 | 1.6524 |
| 0.22 | 1.0 | 3.1542 | 1.0984 |

## 4. Conclusions

The problem of two-dimensional fluid in the prances of thermal and concentration buoyancy effects under the influence of uniform magnetic field applied normal to the flow is formulated and solved numerically. A Galerkin finite element method is adopted to solve the equations governing the flow. The results illustrate the flow characteristics for the velocity, temperature, concentration, skin-friction, Nusselt number, and Sherwood number. The conclusions of the study are as follows

(i) Increasing in the velocity number substantially increase in the Solutal Grashof number.
(ii) Decreasing in the velocity with an increase in the Magnetic parameter.
(iii) Increase in the Permeability of the porous medium parameter with increases in velocity.

(iv) Increasing the Prandtl number substantially decreases the translational velocity and the temperature function.
(v) As the Heat source parameter increases both velocity and temperature decreases.
(vi) As velocity and temperature rises with reduce in the Thermal radiation parameters
(vii) Increase in the Schmidt number the velocity as well as concentration reduce.
(viii) As rise in the Soret number leads to reduce in the velocity and temperature.
(ix) As rise in the Chemical reaction the velocity as well as concentration reduce.

## Acknowledgement
I would like to thank Institute Geethanjali College of Engineering and Technology for unwavering encouragement to do research papers and my co-authors for their collaborative efforts and contributions, their expertise, insightful discussions, and camaraderie have enriched the quality of this study.

## References
[1] Sivaiah, G., Konda Jayarami Reddy, P. Chandra Reddy, and M. C. Raju. "Numerical study of mhd boundary layer flow of a viscoelastic and dissipative fluid past a porous plate in the presence of thermal radiation." *International Journal of Fluid Mechanics Research* 46, no. 1 (2019): 27-38. https://doi.org/10.1615/InterJFluidMechRes.2018020153
[2] Reddy, P. Chandra, K. Venkateswara Raju, M. Umamaheswar, and M. C. Raju. "Buoyancy effects on chemically reactive magnetonanofluid past a moving vertical plate." *Bulletin of Pure & Applied Sciences* 38E, no. 1 (2019): 193-207. https://doi.org/10.5958/2320-3226.2019.00017.1
[3] Reddy, Poli Chandra, M. Umamaheswar, S. Harinath Reddy, and M. C. Raju. "Analytical study of buoyancy effects on MHD visco-elastic fluid past an inclined plate." In *AIP Conference Proceedings*, vol. 2246, no. 1. AIP Publishing, 2020. https://doi.org/10.1063/5.0014572
[4] Meruva, Parvathi, P. Chandra Reddy, P. Roja, A. Leela Ratnam, and M. C. Raju. "Convective heat transfer and mass transfer observations of MHD Cu-water nanofluid in a rotating system." In *AIP Conference Proceedings*, vol. 2246, no. 1. AIP Publishing, 2020. https://doi.org/10.1063/5.0014625
[5] Umamaheswar, M., P. Chandra Reddy, K. Janardhan, M. C. Raju, and G. S. S. Raju. "Unsteady MHD free convective flow of a radiating fluid past an inclined permeable plate in the presence of heat source." In *AIP Conference Proceedings*, vol. 2246, no. 1. AIP Publishing, 2020. https://doi.org/10.1063/5.0014630
[6] Chen, Chien-Hsin. "Combined heat and mass transfer in MHD free convection from a vertical surface with Ohmic heating and viscous dissipation." *International Journal of Engineering Science* 42, no. 7 (2004): 699-713. https://doi.org/10.1016/j.ijengsci.2003.09.002
[7] Mbeledogu, I. U., and A. Ogulu. "Heat and mass transfer of an unsteady MHD natural convection flow of a rotating fluid past a vertical porous flat plate in the presence of radiative heat transfer." *International Journal of Heat and Mass Transfer* 50, no. 9-10 (2007): 1902-1908. https://doi.org/10.1016/j.ijheatmasstransfer.2006.10.016
[8] Pal, Dulal, and Babulal Talukdar. "Buoyancy and chemical reaction effects on MHD mixed convection heat and mass transfer in a porous medium with thermal radiation and Ohmic heating." *Communications in Nonlinear Science and Numerical Simulation* 15, no. 10 (2010): 2878-2893. https://doi.org/10.1016/j.cnsns.2009.10.029
[9] Palani, G., and I. A. A. Abbas. "Free convection MHD flow with thermal radiation from an impulsively-started vertical plate." *Nonlinear Analysis: Modelling and Control* 14, no. 1 (2009): 73-84. https://doi.org/10.15388/NA.2009.14.1.14531
[10] Prakash, J., A. Ogulu, and E. Zhandire. "MHD free convection and mass transfer flow of a micro-polar thermally radiating and reacting fluid with time dependent suction." *Indian Journal of Pure & Applied Sciences* 46 (2008): 679-684.
[11] Suneetha, S., N. Bhaskar Reddy, and V. Ramachandra Prasad. "Radiation and Mass Transfer Effects on MHD Free Convective Dissipative Fluid in the Presence of Heat Source/Sink." *Journal of Applied Fluid Mechanics* 4, no. 1 (2012): 107-113. https://doi.org/10.36884/jafm.4.01.11907
[12] Rao, J. Anand, and R. Srinivasa Raju. "The effects of Hall currents, Soret and Dufour on an unsteady MHO flow and heat transfer along a porous flat plate with mass transfer." *Journal of Energy, Heat and Mass Transfer* 33, no. 4 (2011): 351-372.
[13] Srihari, K., N. Kishan, and J. Anand Rao. "Hall effect on MHD flow and heat transfer along a porous flat plate with mass transfer and source/sink." *Journal of Energy, Heat and Mass Transfer* 30 (2008): 361-376.

[14] Abbas, Zaheer, and Tasawar Hayat. "Radiation effects on MHD flow in a porous space." *International Journal of Heat and Mass Transfer* 51, no. 5-6 (2008): 1024-1033. https://doi.org/10.1016/j.ijheatmasstransfer.2007.05.031
[15] Reddy, B. Prabhakar, and Oluwole D. Makinde. "Newtonian heating effect on heat absorbing unsteady MHD radiating and chemically reacting free convection flow past an oscillating vertical porous plate." *International Journal of Applied Mechanics and Engineering* 27, no. 1 (2022): 168-187. https://doi.org/10.2478/ijame-2022-0011
[16] Reddy, B. Prabhakar, and O. D. Makinde. "Numerical study on heat absorbing MHD radiating and reacting flow past an impulsively moving vertical plate with ramped temperature and concentration with Hall current." *International Journal for Computational Methods in Engineering Science and Mechanics* 23, no. 5 (2022): 383-395. https://doi.org/10.1080/15502287.2021.1977419
[17] Reddy, B. Prabhakar, and O. D. Makinde. "Numerical study on MHD radiating and reacting unsteady slip flow past a vertical permeable plate in a porous medium." *International Journal of Ambient Energy* 43, no. 1 (2022): 6007-6016. https://doi.org/10.1080/01430750.2021.1999323
[18] Reddy, B. Prabhakar, O. D. Makinde, and Alfred Hugo. "A computational study on diffusion-thermo and rotation effects on heat generated mixed convection flow of MHD Casson fluid past an oscillating porous plate." *International Communications in Heat and Mass Transfer* 138 (2022): 106389. https://doi.org/10.1016/j.icheatmasstransfer.2022.106389
[19] Hamrelaine, Salim, Fateh Mebarek-Oudina, and Mohamed Rafik Sari. "Analysis of MHD Jeffery Hamel flow with suction/injection by homotopy analysis method." *Journal of Advanced Research in Fluid Mechanics and Thermal Sciences* 58, no. 2 (2019): 173-186.
[20] Ismail, Atifatul Ismah, Sher Afghan Khan, Parvathy Rajendran, and Erwin Sulaeman. "Effect of cavities in suddenly expanded flow at supersonic mach number." *CFD Letters* 13, no. 9 (2021): 57-71. https://doi.org/10.37934/cfdl.13.9.5771
[21] Bakar, Shahirah Abu, Norihan Md Arifin, and Ioan Pop. "Stability analysis on mixed convection nanofluid flow in a permeable porous medium with radiation and internal heat generation." *Journal of Advanced Research in Micro and Nano Engineering* 13, no. 1 (2023): 1-17. https://doi.org/10.37934/armne.13.1.117